

Quasidistribution of phases in Raman process with weak and strong pumps

Kishore Thapliyal^{1,*} and Jan Peřina^{2,3}

¹*RCPTM, Joint Laboratory of Optics of Palacký University and Institute of Physics of Academy of Science of the Czech Republic, Faculty of Science, Palacký University, 17. listopadu 12, 771 46 Olomouc, Czech Republic*

²*Joint Laboratory of Optics of Palacký University and Institute of Physics of Academy of Science of the Czech Republic, Faculty of Science, Palacký University, 17. listopadu 12, 771 46 Olomouc, Czech Republic*

³*Department of Optics, Faculty of Science, Palacký University, 17. listopadu 12, 771 46 Olomouc, Czech Republic*

(Dated:)

Nonclassicality is studied through a quasidistribution of phases for the Raman process under both weak and strong pump conditions. In the former case, the solution is applicable to both resonant and off-resonant Raman processes, while strong classical pump is assumed at resonance. Under weak pump conditions (i.e., in a complete quantum treatment), the phase difference of phases described by single nonclassical modes is required to be filtered to describe a regular distribution function, which is not the case with strong pump. Compound Stokes-phonon mode shows nonclassical features of phases in both weak and strong pumping, which effect is similar to that for compound pump-phonon (Stokes-anti-Stokes) mode with weak (strong) pump. While anti-Stokes-phonon mode is observed to be classical and coherence conserving in strong pump case, pump-Stokes mode shows similar behavior in a special case in quantum treatment.

I. INTRODUCTION

Nonclassical states, having negative values of (multimode) Glauber-Sudarshan $P(\{\alpha_j\})$ ($\{\alpha_j\} = \{\alpha_1, \alpha_2, \dots, \alpha_n\}$) quasidistribution function [1, 2], are significant resource in multifaceted quantum information processing and technology, namely quantum communication [3], computational supremacy [4], metrology [5], machine learning [6], sensing [7], simulation [8], game theory [9], etc. Independently, studies related to quantum phase have also garnered attention over the past few decades (see [10] for review). Recently, nonclassicality in the phase is also studied by isolating the role of quantum phase from the classical phase in optomechanical system [11]. Interestingly, when having quasidistribution $P(\{\alpha_j\})$ of complex amplitudes $\alpha_j = |\alpha_j| \exp(i\phi_j)$, integrating over the moduli of real amplitudes, we can obtain a quasidistribution $\Theta(\{\phi_j\})$ of phases ϕ_j . In the classical region, it is regular, while in the quantum region it may be singular. However, in [12] a procedure has been suggested to show that one can obtain a regular distribution also in the quantum region provided that some phase differences of the phases are filtered.

In what follows, we study here the effect of nonclassicality on values of phase differences allowed to describe the quasidistribution of phase difference in case of both resonant and off-resonant Raman processes. Specifically, we illustrate this using the nonlinear optical process of Raman scattering in finite-time approximation with weak pumping and in parametric approximation with strong coherent classical pumping. We mainly analyze conditions for the distribution of phase differences, whereas their forms are given in [12].

II. QUASIDISTRIBUTION OF PHASES IN RAMAN PROCESS

We will be considering two scenarios: weak and strong pumps. In the first case an approximate perturbation solution using a complete quantum treatment is obtained which is applicable for both resonant and off-resonant Raman processes [13, 14]. In contrast, in the latter case of strong coherent classical pumping, an exact analytic solution is possible [15].

As the quasidistribution $P(\{\alpha_j\})$ can be described in terms of normal ordered characteristic function $C(\{\beta_j\})$, it allows us to describe quasidistribution of phases $\Theta(\{\phi_j\})$ directly in terms of characteristic function as [12]

$$\Theta(\{\phi_j\}) = \frac{1}{\pi^{2n}} \mathcal{P} \int \prod_{j=1}^n \frac{C(\{\beta_j\})}{(\beta_j \exp(-i\phi_j) - \text{c.c.})} d^2\beta_j, \quad (1)$$

*Email:kishore.thapliyal@upol.cz

where \mathcal{P} means the principal value of the integral, and $\{\beta_j\} = \{\beta_1, \beta_2, \dots, \beta_n\}$ are parameters of the characteristic function. Time evolution of the normal ordered characteristic function in both weak and strong pump cases can be described in the Gaussian form as

$$C(\{\beta_j\}, t) = \left\langle \exp \left\{ \sum_{j < k = \mathcal{S}} \left[-(B_j(t) - |C_j(t)| \cos \eta_j) |\beta_j|^2 + 2 |\beta_j \beta_k| (|D_{jk}(t)| \cos \epsilon_{jk} + |\bar{D}_{jk}(t)| \cos \bar{\epsilon}_{jk}) \right] \right\} \right\rangle \quad (2)$$

in terms of quantum noise functions [16] defined as $B_j = \langle \Delta a_j^\dagger \Delta a_j \rangle$, $C_j = \langle (\Delta a_j)^2 \rangle$, $D_{jk} = \langle \Delta a_j \Delta a_k \rangle$, and $\bar{D}_{jk} = -\langle \Delta a_j^\dagger \Delta a_k \rangle$ with $\{\beta_j\} = \{\beta_{\mathcal{S}}\}$. Here, $\eta_j = \arg(C_j)$, $\epsilon_{jk} = \arg(D_{jk})$, and $\bar{\epsilon}_{jk} = \arg(\bar{D}_{jk})$. The set \mathcal{S} is assumed ordered being $\mathcal{S} = \{L, S, V, A\}$ and $\mathcal{S} = \{S, V, A\}$ in case of weak and strong pump cases, respectively.

The single-mode nonclassicality is characterized by $s_i = B_i/|C_i| < 1$. This parameter $s_i > \cos \eta_i$ in turn also determines the bound of the phase corresponding to nonclassical region [12]. Similarly, we lack a classical description in two-mode nonclassical region if $q_{jk} = (B_j - |C_j| \cos \eta_j)(B_k - |C_k| \cos \eta_k) / (|D_{jk}| + |\bar{D}_{jk}|)^2 < 1$. This parameter also determines the corresponding threshold value of phase in the nonclassical region [12] as $1 - q_{jk} < \sin^2 \Psi_{jk}$, where $\Psi_{jk} = \epsilon_{jk} - \phi_j - \phi_k$. The phases Ψ_{jk} and $\bar{\Psi}_{jk} = \bar{\epsilon}_{jk} + \phi_j - \phi_k$ fulfill

$$|D_{jk}|^2 \sin^2 \Psi_{jk} + |\bar{D}_{jk}|^2 \sin^2 \bar{\Psi}_{jk} + 2 |D_{jk}| |\bar{D}_{jk}| (1 - \cos \Psi_{jk} \cos \bar{\Psi}_{jk}) - (1 - q_{jk}) (|D_{jk}| + |\bar{D}_{jk}|)^2 > 0.$$

The corresponding phase distributions are given in [12] in a canonical form in dependence on q_{jk} .

A. Raman process with weak pump

Firstly, we begin with Raman process with weak pump conditions. The perturbative analytic form of quantum noise terms in the characteristic function (2) in this case is reported in Appendix A. We are interested in the off-resonant Raman process [13] where the dynamics is dependent upon two frequency detuning parameters, particularly $\Delta\omega_1 = (\omega_S + \omega_V - \omega_L)$ and $\Delta\omega_2 = (\omega_L + \omega_V - \omega_A)$ as detuning parameters in Stokes and anti-Stokes generation processes, respectively. Here, ω_L , ω_S , ω_A , and ω_V correspond to pump, Stokes, anti-Stokes, and phonon mode frequencies, respectively.

We have considered two limiting cases, $\Delta\omega_1 = \Delta\omega_2 = \delta_1$ (related to radiation modes) and $\Delta\omega_1 = -\Delta\omega_2 = \delta_2$ (related to vibrational mode), which we will refer to Case 1 and Case 2, respectively. In Case 1, the value of s_i parameter for pump and phonon modes are

$$\begin{aligned} s_{L1} &= \frac{2p \sin^2 \frac{\delta_1 t}{2}}{\Lambda_1} \sqrt{\frac{I_A}{I_S}} > \cos \eta_{L1}, \\ s_{V1} &= \frac{(I_L + p^2 I_A)}{p \sqrt{I_S I_A}} > \cos \eta_{V1}. \end{aligned} \quad (3)$$

Here and in what follows, $\Lambda_i^2 = (\delta_i^2 t^2 + 4 \sin^2 \frac{\delta_i t}{2} - 2 \delta_i t \sin \delta_i t)$, intensity of each mode $I_i = |\xi_i|^2$, $p = \frac{|\chi|}{|g|}$, where g and χ are Stokes and anti-Stokes coupling constants, respectively. Also, $\cos \eta_{L1} = -2\Re(\chi g^* \{2 \sin^2 \frac{\delta_1 t}{2} + i(\delta_1 t - \sin \delta_1 t)\} \exp\{i(\phi_A + \phi_S - 2\omega_L t)\}) / (|\chi| |g| \Lambda_1)$. Assuming coupling constant real and in the limits of zero detuning (corresponding to resonant Raman process), $\eta_{L1} = -\phi_S - \phi_A + 2\omega_L t$ is solely determined by the phase of Stokes and anti-Stokes modes and pump frequency. Similarly, $\cos \eta_{V1} = -\Re(\chi g \exp\{i(\phi_A - \phi_S - 2\omega_V t + \delta_1 t)\}) / (2|\chi| |g|)$ with ω_V as the phonon frequency, which reduces to $\eta_{V1} = \phi_S - \phi_A + 2\omega_V t$ for real coupling constants for resonant Raman process. Similarly, in Case 2, the same witness turns out to be

$$\begin{aligned} s_{L2} &= p \sqrt{\frac{I_A}{I_S}} > \cos \eta_{L2}, \\ s_{V2} &= \frac{2 \sin^2 \frac{\delta_2 t}{2} (I_L + p^2 I_A)}{p \Lambda_2 \sqrt{I_S I_A}} > \cos \eta_{V2}. \end{aligned} \quad (4)$$

In this case, $\cos \eta_{L2} = -\Re(\chi g^* \exp\{i(\phi_S + \phi_A - 2\omega_L t - \delta_2 t)\}) / (2|\chi| |g|)$ and $\cos \eta_{V2} = -2\Re(\chi g \{2 \sin^2 \frac{\delta_2 t}{2} + i(\delta_2 t - \sin \delta_2 t)\} \exp\{i(\phi_A - \phi_S - 2\omega_V t)\}) / (|\chi| |g| \Lambda_2)$, which are same but out of phase with η_{L1} and η_{V1} for real coupling constants in resonant Raman process, respectively.

One can clearly verify that $\lim_{\delta_1 \rightarrow 0} s_{L1} = s_{L2}$ and $\lim_{\delta_2 \rightarrow 0} s_{V2} = s_{V1}$, which represents results for Raman process at resonance (using $\lim_{\delta_i \rightarrow 0} 2 \sin^2 \frac{\delta_i t}{2} / \Lambda_i = 1$). As the Cases 1 and 2 and small detuning fully determine the approximation

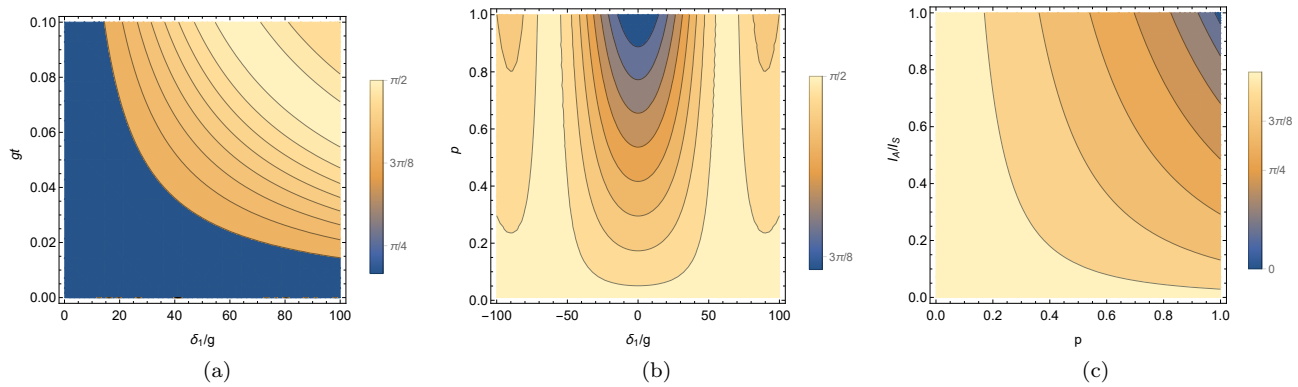


Figure 1: (Color online) Dependence of bound for η_{L1} (which is given by the value of $\cos^{-1} s_{L1}$) on different parameters, i.e., detuning parameter and (a) rescaled time and (b) the ratio of anti-Stokes and Stokes coupling constants; (c) dependence of s_{L2} on rescaled time and the ratio of anti-Stokes and Stokes coupling constants. The plots are obtained by choosing $I_S = 6$ and $I_A = 1$ (wherever needed). All the quantities in this figure and rest of the figures are dimensionless.

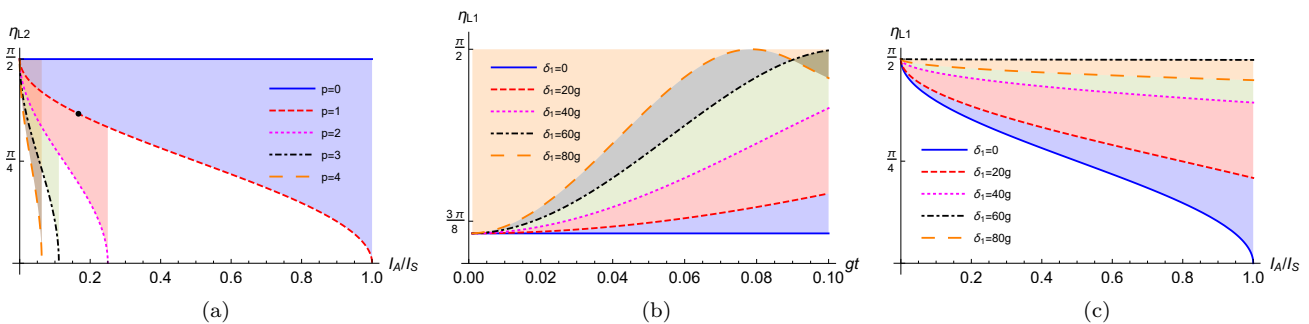


Figure 2: (Color online) (a) Dependence of η_{L2} bound (applicable for resonant Raman scattering, too) on rescaled time and p . Dependence of s_{L1} on (b) rescaled time and (c) the ratio of anti-Stokes and Stokes intensities for different values of detuning parameter. The allowed values of phase difference are shown as the shaded region. We have chosen $I_S = 6$ and $p = 1$. For the point marked in (a) the effect of frequency detuning parameter is illustrated in (b), while similar variation for the corresponding line is shown in (c).

with the ratios of coupling constants and intensities $\cos \eta_L < s_{L2}$ and $\cos \eta_V < s_{V1}$. Note that the obtained parameters are independent of the initial phonon numbers. It is also easy to check in case of spontaneous process that the parameters cannot be defined for phonon mode. Further, it is safe to assume in case of stimulated process that $\frac{I_A}{I_S} \ll 1$ and $p \approx 1$, and thus the sum of the phases of the Stokes and anti-Stokes modes is described by a generalized quasiprobability distribution. However, feasibility of describing the regular phase distribution for the difference of the phases for resonant Raman process depends on $s_V = I_L / (p\sqrt{I_S I_A}) + s_L$, which is dominated by the first term due to strong pump intensity, and thus it shows classical behavior. Variation of obtained bound of phase difference for pump mode in Case 1 for $\eta_{L1} = \cos^{-1} s_{L1}$ is shown in Fig. 1. Both time evolution and detuning parameter enforce filtering of phase difference to allow a regular distribution function in this case (Fig. 1 (a)-(b)). In contrast, ratio of anti-Stokes and Stokes coupling constants as well as the intensity, however, diminish this filtering (Fig. 1 (b)-(c)).

The bound of phase difference in case of pump mode in Case 2 is also applicable to resonant Raman scattering. Variation of bound for η_{L2} with the ratio of anti-Stokes and Stokes coupling constants (for different Raman active materials [17]) as well as intensity is shown in Fig. 2 (a). We have marked a point on Fig. 2 (a) and shown its time evolution for off-resonant Raman process for η_{L1} in Fig. 2 (b). The similar variation of the line containing the point with the ratio of anti-Stokes and Stokes intensity and frequency detuning is shown in Fig. 2 (c). Both increasing time evolution and frequency detuning require more filtering, while $\frac{I_A}{I_S}$ has the opposite effect.

In the present case, q_{ij} parameter based on two-mode nonclassicality is used further to study filtering of phase difference in such cases. A much simpler form is $q_{SV} \approx |g|^2 t^2 I_L \text{sinc}^2 \delta_i t$ which can be obtained in the spontaneous case. The simplified form is less than 1 imposing condition for short-time limit [13] $|g| t \sqrt{I_L} < 1$ and assuming $\delta_i t \ll 1$. Thus, q_{SV} can be observed in good agreement with the complete expression in the short-time and small detuning limits as

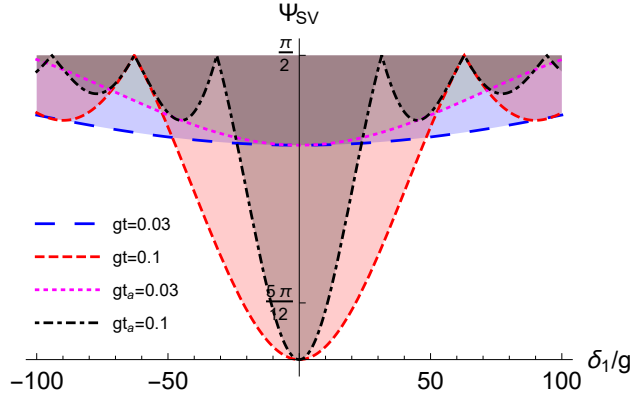


Figure 3: (Color online) Variation of complete analytic solution and simplified approximate solution (with a in the subscript in the plot legends) for Ψ_{SV} parameters with frequency detuning. The allowed values of phase are shown as the shaded region. The results are obtained for spontaneous case with $I_L = 10$ and $p = 1$. Similar behavior was observed for Ψ_{LV} in the stimulated case.

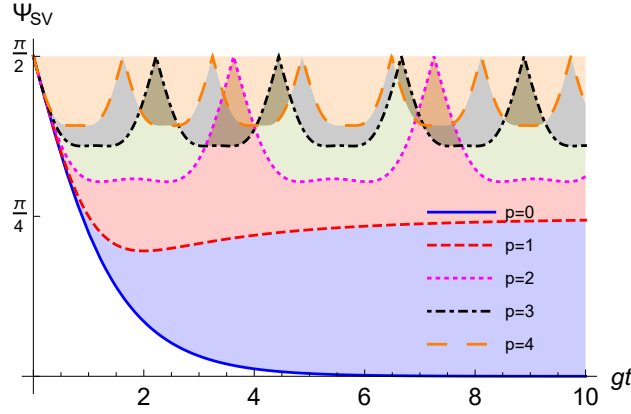


Figure 4: (Color online) Time evolution of Ψ_{SV} parameter for different values of the ratio of anti-Stokes and Stokes coupling constants. This parameter filters the value of $\Psi_{SV} = -(\Phi_L - \omega_V t)$ (shown as the shaded region). Note that the quantity shown in the plot coincides with $\Psi_{SA} = -(2\Phi_L - \omega_A t)$.

shown in Fig. 3, where we have exhibited the allowed region for phase Ψ_{SV} in different cases by different colors. Due to the complex structure of bound for the phase difference parameter in off-resonant case, we report here corresponding parameter for zero detuning as $\Psi_{SV} = \arg \left[-gte^{-it(\omega_b + \omega_c)} \left(g^* t \sqrt{I_S I_V} e^{i(\phi_S + \phi_V)} + 2\chi t \sqrt{I_A I_V} e^{i(\phi_A - \phi_V)} - 2i\sqrt{I_L} e^{i\phi_L} \right) \right]$. The simplified approximate solution is marked with 'a' in the subscript in Fig. 3. Clearly, the approximate solution always gives the narrower region than that is shown by the complete analytic solution. Similarly, in the partial stimulated case (i.e., $I_A \neq 0 = I_S$), $q_{LV} \approx |g|^2 (t^2 I_L + p^2 t^2 I_A) \text{sinc}^2 \delta_i t$, which qualitatively concludes the same as for Ψ_{SV} in Fig. 3. The corresponding behavior for $\Psi_{LV} = \arg \left[-e^{-it(\omega_V + \omega_L)} \left(\left\{ |g|^2 + |\chi|^2 \right\} t^2 \sqrt{I_L I_V} e^{i(\phi_L + \phi_V)} - 2i\chi t \sqrt{I_A} e^{i\phi_A} \right) \right]$ was obtained for resonant Raman stimulated process.

While for pump-Stokes case, we have obtained in partial stimulated cases that $q_{LS} = 1$ if $I_A \neq 0 = I_S$, it is $q_{LS} = 0$ for $I_S \neq 0 = I_A$. This means that the compound pump-Stokes mode is classical in the former case, coherence from the laser mode is directly transferred to the Stokes mode and the wave distribution is proportional to the Dirac δ -function, as $B_L B_S - |\bar{D}_{LS}|^2 = 0$ and $C_L = C_S = D_{LS} = 0$. In the latter case, there is no filtering of phase differences as $B_L = C_L = 0$ and $D_{LS} \neq 0 \neq B_S$. Here, $\sin \Psi_{LS} = -2\Re \left\{ \left(2 \sin^2 \frac{\delta_j t}{2} + i(\delta_j t - \sin \delta_j t) \right) \exp \left\{ -i(\phi_S + \phi_L - (\omega_L + \omega_S)t) \right\} \right\} / \Lambda_j$ in both Case 1 and Case 2. Similarly, one can calculate $\sin \bar{\Psi}_{LS} = \Re (\chi g^* \exp \{i(\phi_A - \phi_L - (\omega_L - \omega_S)t)\}) / (|\chi| |g|)$ and $\sin \bar{\Psi}_{LS} = \Re (\chi g^* \exp \{i(\phi_A - \phi_L - (\omega_L - \omega_S - \delta_2)t)\}) / (|\chi| |g|)$ in Cases 1 and 2, respectively, to verify phase relations.

B. Raman process with strong pump

An exact closed form analytic solution and characteristic function [15] can be obtained for strong pump resonant Raman process. The solution and its brief detail are given in Appendix B. In this section, we study the phase properties of the Raman process with strong coherent classical pump. Specifically, the filtering in phase distributions cannot be studied from the signatures of single-mode nonclassicality criterion as all noise parameters $C_i = 0$. Thus, using two-mode criterion we obtained

$$q_{SV} = q_{SA} = \frac{\left((p^2-1) \sin^2(gt\sqrt{p^2-1}) + 2p^2 \sin^4\left(\frac{gt\sqrt{p^2-1}}{2}\right) \right)}{\left(p^2 - \cos(gt\sqrt{p^2-1}) \right)^2}, \quad (5)$$

$$q_{VA} = 1.$$

Here, $\sin \Psi_{SV} = -\Im(g) \cos(\Phi_L - \omega_V t) + \Re(g) \sin(\Phi_L - \omega_V t) / |g|$ with Φ_L as the phase of the strong classical pump beam, which becomes $\Psi_{SV} = -\Phi_L + \omega_V t$ for real coupling constants. Similarly, $\sin \Psi_{SA} = -\Im(\chi g \exp\{2i\Phi_L - i\omega_A t\}) / (|\chi| |g|)$ which becomes $\Psi_{SA} = -2\Phi_L + \omega_A t$ for real coupling constants.

Similarly, it is possible to calculate $1 - q_{jk} < \sin^2 \Psi_{jk}$ as $\sin \Psi_{VA} = -\Im(\chi^* \exp\{-i\Phi_L + i(\omega_A - \omega_V)t\}) / |\chi|$, which becomes $\Psi_{VA} = \Phi_L - (\omega_A - \omega_V)t$ for real coupling constants. As $q_{VA} = 1$ in this case, all the values of Ψ_{VA} are allowed. Note that although we are using the same coupling constant parameters in both weak and strong pump cases, pump amplitude is originally included in the coupling amplitudes (i.e., in the latter, these constants will be $\sqrt{I_L}$ times the corresponding constants in the former case). For classical strong pumping, the compound anti-Stokes-phonon mode corresponds with the process of frequency-conversion conserving coherence ($B_A B_V - |\bar{D}_{VA}|^2 = 0$) and the wave distribution is proportional to the Dirac δ -function. In short interaction times there is no quantum noise in the anti-Stokes mode, which has a tendency to conserve coherence, being attenuated. However, for strong pumping and large interaction times also in the anti-Stokes mode the quantum noise is developed.

In Fig. 4, time evolution of Ψ_{SV} (and thus Ψ_{SA} , too) causes filtering of the phase of the pump mode with respect to the frequency of the phonon mode and shows that for different values of p the phase distribution becomes singular at different rescaled times. Further, from the figure it can be seen that with increase in the anti-Stokes coupling with respect to Stokes coupling allowed range of values of Ψ_{SV} (and similarly Ψ_{SA}) decreases. For instance, in case of zero anti-Stokes coupling (which can be assumed in the weak pump conditions in the present case) there is no filtering observed after certain value of rescaled time. In contrast, with higher values of anti-Stokes coupling with respect to Stokes coupling the pump phases are filtered to a smaller range of values around $\frac{\pi}{2}$.

III. CONCLUSIONS

Quasidistribution of phases for the Raman process is obtained from corresponding Glauber-Sudarshan $P(\{\alpha_j\})$ quasidistribution function by integrating over moduli of complex amplitudes. Thus obtained unnormalized quasidistribution of phases contains signatures of nonclassicality. Here, we have studied the effect of these nonclassical behavior in the Raman process under both weak and strong pump conditions on corresponding phase properties. The weak pump case is studied by performing complete quantum treatment to obtain perturbative solution which is applicable to both resonant and off-resonant Raman processes. In contrast, with parametric approximation, i.e., strong classical pump, an exact solution is possible, which is obtained only for resonant Raman process.

The single-mode nonclassicality is observed only with a complete quantum treatment, and the phase differences of phases described by single nonclassical modes are required to be filtered to describe a regular distribution function. The compound anti-Stokes-phonon mode is observed to be classical and coherence is conserved in strong pump case and corresponding wave distribution can be described by Dirac δ -functions. Similar behavior is observed in special case in pump-Stokes mode with weak pump. Compound Stokes-phonon mode shows nonclassical features of phases with both weak and strong pumping, which behavior is similar to pump-phonon (Stokes-anti-Stokes) mode with weak (strong) pump.

The present study shows the effect of nonclassicality present in the output modes of the Raman process on corresponding phase properties and will be helpful in understanding the behavior observed in the experiments. In particular, in [11], the authors illustrated possibility to distinguish classical and quantum phases in optomechanical interference experiment with weak coupling and for small photon numbers and low temperature. Our suggestion of the interference experiment [12] for obtaining the presented nonclassical phase effects has to follow such conditions.

Acknowledgement: Authors acknowledge the financial support from the Operational Programme Research, Development and Education - European Regional Development Fund project no. CZ.02.1.01/0.0/0.0/16 019/0000754

of the Ministry of Education, Youth and Sports of the Czech Republic.

-
- [1] R. J. Glauber, Phys. Rev. **131**, 2766 (1963).
[2] E. C. G. Sudarshan, Phys. Rev. Lett. **10**, 277 (1963).
[3] N. Gisin and R. Thew, Nature Photonics **1**, 165 (2007).
[4] A. W. Harrow and A. Montanaro, Nature **549**, 203 (2017).
[5] V. Giovannetti, S. Lloyd, and L. Maccone, Nature Photonics **5**, 222 (2011).
[6] J. Biamonte, P. Wittek, N. Pancotti, P. Rebentrost, N. Wiebe, and S. Lloyd, Nature **549**, 195 (2017).
[7] C. L. Degen, F. Reinhard, and P. Cappellaro, Rev. Mod. Phys. **89**, 035002 (2017).
[8] I. M. Georgescu, S. Ashhab, and F. Nori, Rev. Mod. Phys. **86**, 153 (2014).
[9] J. Eisert, M. Wilkens, and M. Lewenstein, Phys. Rev. Lett. **83**, 3077 (1999).
[10] V. Peřinová, A. Lukš, and J. Peřina, *Phase in Optics* (World Scientific, 1998).
[11] F. Armata, L. Latmiral, I. Pikovski, M. R. Vanner, Č. Brukner, and M. Kim, Phys. Rev. A **93**, 063862 (2016).
[12] J. Peřina and J. Křepelka, Optics Communications **437**, 373 (2019).
[13] K. Thapliyal and J. Peřina, Physics Letters A **383**, 2011 (2019).
[14] K. Thapliyal, A. Pathak, B. Sen, and J. Peřina, Optics Communications **444**, 111 (2019).
[15] A. Pieczonková and J. Peřina, Czech. J. Phys. B **31**, 837 (1981).
[16] J. Peřina, *Quantum Statistics of Linear and Nonlinear Optical Phenomena* (Kluwer Academic, Dordrecht-Boston, 1991).
[17] C. A. Parra-Murillo, M. F. Santos, C. H. Monken, and A. Jorio, Phys. Rev. B **93**, 125141 (2016).

Appendix A: Finite time coefficient of characteristic function

In the present case, the obtained quantum noise function terms are as follows [13]

$$\begin{aligned}
B_L(t) &= \frac{2|\chi|^2|\xi_A|^2(1-\cos\delta_i t)}{\delta_i^2}, \\
B_S(t) &= \frac{2|g|^2|\xi_L|^2(1-\cos\delta_i t)}{\delta_i^2}, \\
B_V(t) &= B_L(t) + B_S(t), \\
C_L(t) &= \frac{2\xi_S\xi_A\chi g^* e^{-it(\delta_i+2\omega_L)} \left(\pm 2\sin^2\left(\frac{\delta_i t}{2}\right) - i(\sin\delta_1 t - \delta_1 t e^{i\delta_1 t}) \right)}{\delta_i^2}, \\
C_V(t) &= \frac{2\xi_S^*\xi_A\chi g e^{it(\delta_i-2\omega_V)} \left(\mp 2\sin^2\left(\frac{\delta_i t}{2}\right) + i(\sin\delta_2 t - \delta_2 t e^{-i\delta_2 t}) \right)}{\delta_i^2}, \\
D_{LS}(t) &= \frac{\xi_S\xi_L|g|^2 e^{-it(\omega_L+\omega_S)} \left(-2\sin^2\left(\frac{\delta_i t}{2}\right) - i(\sin\delta_i t - \delta_i t) \right)}{\delta_i^2}, \\
D_{LV}(t) &= \frac{2i\chi\xi_A \sin\left(\frac{\delta_i t}{2}\right) e^{-it(\omega_L+\omega_V \pm \frac{\delta_i}{2})}}{\delta_i} - \frac{\xi_L\xi_V e^{-it(\omega_L+\omega_V)} \left((|g|^2+|\chi|^2) \left\{ 2\sin^2\left(\frac{\delta_i t}{2}\right) + i(\sin\delta_i t - \delta_i t) \right\} - 2i|\chi|^2(\sin\delta_1 t - \delta_1 t) \right)}{\delta_i^2}, \\
D_{LA}(t) &= \frac{\xi_L\xi_A|\chi|^2 e^{-it(\omega_L+\omega_A)} \left(-2\sin^2\left(\frac{\delta_i t}{2}\right) \mp i(\sin\delta_i t - \delta_i t) \right)}{\delta_i^2}, \\
D_{SV}(t) &= \frac{2i\chi\xi_L \sin\left(\frac{\delta_i t}{2}\right) e^{-it\left(\frac{\delta_i}{2}+\omega_S+\omega_V\right)}}{\delta_i} + \frac{\xi_S\xi_V|g|^2 e^{-it(\omega_S+\omega_V)} \left(-2\sin^2\left(\frac{\delta_i t}{2}\right) + i(\sin\delta_i t - \delta_i t) \right)}{\delta_i^2} \\
&\quad + \frac{2\xi_V^*\xi_A\chi g \left(\mp 2\sin^2\left(\frac{\delta_i t}{2}\right) + i(\sin\delta_2 t - \delta_2 t e^{-i\delta_2 t}) \right) e^{-it(\omega_S+\omega_V-\delta_i)}}{\delta_i^2}, \\
D_{SA}(t) &= \frac{\xi_L^*\chi^* g e^{-it(\omega_S+\omega_A)} \left(-2\sin^2\left(\frac{\delta_i t}{2}\right) - 4\sin^2\left(\frac{\delta_2 t}{2}\right) e^{i\delta_2 t} - i(\sin\delta_1 t - \delta_1 t) \right)}{\delta_i^2}, \\
D_{VA}(t) &= \frac{\xi_V\xi_A|\chi|^2 e^{-it(\omega_V+\omega_A)} \left(-2\sin^2\left(\frac{\delta_i t}{2}\right) \mp i(\sin\delta_i t - \delta_i t) \right)}{\delta_i^2}, \\
\bar{D}_{LS}(t) &= \frac{4\chi^*g\xi_L\xi_A^* \sin^2\left(\frac{\delta_i t}{2}\right) e^{-it(\delta_2-\omega_L+\omega_S)}}{\delta_i^2}.
\end{aligned} \tag{A.1}$$

The rest of the terms in Eq. (2) are zero. Here, $\delta_1 \neq 0$ and $\delta_2 = 0$ ($\delta_1 = 0$ and $\delta_2 \neq 0$) correspond to Case 1 (Case 2).

Appendix B: Strong-pump solution (some features)

Quantum noise fluctuation terms in the characteristic function can be written as [15]

$$\begin{aligned}
B_V &= \frac{|g|^2 \sin^2(t\sqrt{|\chi|^2 - |g|^2})}{(|\chi|^2 - |g|^2)}, \\
B_A &= \frac{|\chi|^2 |g|^2 (1 - \cos(t\sqrt{|\chi|^2 - |g|^2}))^2}{(|\chi|^2 - |g|^2)^2}, \\
B_S &= B_V + B_A, \\
D_{SA} &= \frac{-\chi g (1 - \cos(t\sqrt{|\chi|^2 - |g|^2})) \{|\chi|^2 - |g|^2 \cos(t\sqrt{|\chi|^2 - |g|^2})\} \exp(2i\Phi_L - i(\omega_A + \omega_S)t)}{(|\chi|^2 - |g|^2)^2}, \\
D_{VS} &= \frac{ig \sin(t\sqrt{|\chi|^2 - |g|^2}) \{|\chi|^2 - |g|^2 \cos(t\sqrt{|\chi|^2 - |g|^2})\} \exp(i\Phi_L - i(\omega_V + \omega_S)t)}{(|\chi|^2 - |g|^2)^{3/2}}, \\
\bar{D}_{VA} &= \frac{i|g|^2 \chi^* \sin(t\sqrt{|\chi|^2 - |g|^2}) (1 - \cos(t\sqrt{|\chi|^2 - |g|^2})) \exp(-i\Phi_L - i(\omega_V - \omega_A)t)}{(|\chi|^2 - |g|^2)^{3/2}},
\end{aligned} \tag{B.1}$$

while the rest of the terms are zero.